HHS Public Access

Author manuscript

Oncogene. Author manuscript; available in PMC 2024 May 15.

Published in final edited form as:

Oncogene. 2020 February ; 39(8): 1784–1796. doi:10.1038/s41388-019-1105-y.

NER-factor DDB2 regulates HIF1α and hypoxia-response genes in HNSCC

Prashant V. Bommi[1,3], **Vaibhav Chand**[2], **Nishit K. Mukhopadhyay**[2], **Pradip Raychaudhuri**[2], **Srilata Bagchi**[1]

[1]Department of Oral Biology, College of Dentistry, University of Illinois at Chicago, 801 S, Paulina Street, Chicago, IL 60612, USA

[2]Department of Biochemistry and Molecular Genetics, University of Illinois at Chicago, 900 S Ashland Avenue, Chicago, IL 60607, USA

[3]Present address: Department of Clinical Cancer Prevention, University of Texas MD Anderson Cancer Center, Biological Sciences Research Building (BSRB), 6767 Bertner Ave, Houston, TX, USA

Abstract

Cancers in the oral/head & neck region (HNSCC) are aggressive due to high incidence of recurrence and distant metastasis. One prominent feature of aggressive HNSCC is the presence of severely hypoxic regions in tumors and activation of hypoxia-inducible factors (HIFs). In this study, we report that the XPE gene product DDB2 (damaged DNA binding protein 2), a nucleotide excision repair protein, is upregulated by hypoxia. Moreover, DDB2 inhibits HIF1α in HNSCC cells. It inhibits HIF1α in both normoxia and hypoxia by reducing mRNA expression. Knockdown of DDB2 enhances the expression of angiogenic markers and promotes tumor growth in a xenograft model. We show that DDB2 binds to an upstream promoter element in the *HIF1A* gene and promotes histone H3K9 trimethylation around the binding site by recruiting Suv39h1. Also, we provide evidence that DDB2 has a significant suppressive effect on expression of the endogenous markers of hypoxia that are also prognostic indicators in HNSCC. Together, these results describe a new mechanism of hypoxia regulation that opposes expression of *HIF1A* mRNA and the hypoxia-response genes.

Introduction

Hypoxia is a common occurrence during embryonic development, as well as, in pathophysiological conditions such as tumor growth, ischemia, stroke, and wound healing [1–3]. Hypoxia condition signifies severe oxygen deprivation (<2% O_2). It is observed in a wide range of human malignancies such as in oral/head & neck region (HNSCC), breast

✉Pradip Raychaudhuri, pradip@uic.edu, Srilata Bagchi, sbagchi@uic.edu.

Compliance with ethical standards

Conflict of interest The authors declare that they have no conflict of interest.

Supplementary information The online version of this article (https://doi.org/10.1038/s41388-019-1105-y) contains supplementary material, which is available to authorized users.

cancer, uterine cervical cancer, pancreatic cancer, brain tumors, sarcomas, and malignant melanomas [4–7]. Hypoxic condition in cancer is triggered due to hyper-proliferative nature of cancer cells leading to short supply of nutrients and abnormal vascularization. Hypoxia induces transcription of several genes involved in EMT and metabolic reprogramming through stabilization and induction of hypoxia-inducible transcription factors (HIFs) [8, 9]. Hypoxic tumor microenvironment enhances the survival ability of tumor cells by promoting colonization of cancer stem cells and strongly influencing response to therapeutic drugs [10, 11].

Hypoxia-inducible factor 1α (HIF1α), a heterodimeric basic helix-loop-helix PAS domain transcription factor, is the master regulator of hypoxic response (reviewed in [12]). HIF1α protein has a very short half-life (<5 min) [13]. HIF1α proteolysis in normoxia (21% O_2) is triggered by hydroxylation of key proline residues in its conserved oxygen dependent degradation domain by specific prolylhydroxylases (PHDs) [14]. This modification is crucial and necessary for binding to the tumor suppressor Von Hippel–Lindau (VHL). VHL is the recognition component of E3 ubiquitin ligase that targets HIF1α for poly-ubiquitination and destruction through 26S proteasome. As oxygen levels fall below 8%, HIF-α protein is stabilized, and it translocates to nucleus, where it dimerizes with constitutively expressing HIF-β (ARNT), binds to hypoxia regulated elements and activates transcription of over 150 genes by interacting with co-activators such as p300/CBP (reviewed in [8]). Surprisingly, the stabilization of HIF1α at low oxygen (hypoxia) involves reactive oxygen species (ROS). Several studies indicated that hypoxia increases intracellular ROS through mitochondrial mechanisms [15]. Chandel et al. demonstrated that treatment of cells with decreasing levels of oxygen (5, 3, and 1% O_2) caused progressive increase in the levels of cytosolic ROS (hydrogen peroxide) involving the mitochondrial electron transport chain, leading to increase in the levels of HIF1α [16]. Inhibition of hypoxia-induced ROS caused inhibition of HIF1α. Binding of HIF1α to p300/CBP is reported to be dependent on hydroxylation of asparagine residue (N-803) in C-terminal of HIF1α [17, 18]. Other posttranslational modifications such as phosphorylation, acetylation, sumoylation, S-nitrosylation, and neddylation have been reported that promote differential activity of HIF1α [19–25]. While higher HIF1α activity has been traditionally attributed to stabilization of the protein, recent reports indicate that HIF1α expression can be selectively controlled also at the levels of transcription. Two reports show that HIF1α mRNA is induced by NF-κB upon hypoxia [26, 27]. Moreover, cells with activated PI3K-AKT-mTOR signaling, a common feature of cancer cells, were found to promote HIF1α translation rates resulting in increased protein levels and activity of HIF1α [17].

Damaged DNA binding protein 2 (DDB2) is a multi-functional protein encoded by nucleotide excision repair (NER) gene, Xeroderma Pigmentosum complementation group E [28–30]. In addition to its role in NER, DDB2 possesses DNA-lesion independent transcriptional regulatory function. Several reports demonstrated how DDB2 is involved in the regulation of tumor promoting genes. For example, the DDB2 knockout keratinocytes show deficiency in senescence resulting from a lack of ROS accumulation [31]. DDB2 transcriptionally represses the anti-oxidant genes MnSOD [32]. Recent studies show that DDB2 is a potent inhibitor of metastasis in colon cancer, coinciding with its ability to repress expression of pro-EMT genes, SNAIL and ZEB1, and pro-angiogenic factor VEGF

gene [33]. In addition, DDB2 was found to repress the anti-apoptotic gene, BCL2, in human ovarian cancer cells [34]. Overexpression of DDB2 was found to inhibit the self-renewal property and tumorigenicity of ovarian CSCs by suppressing the NF-κB pathway and the stem cell marker Nanog [35]. DDB2-overexpression enhanced TGFβ signal transduction and increased the responsiveness of ovarian cancer cells to TGFβ-induced growth inhibition by downregulating the inhibitor of TGFβ pathway signaling [36]. These various functions of DDB2 converge on inhibiting cancer-promoting events. Our recent studies show that DDB2 represses EMT-regulatory genes in HNSCC [6].

Interestingly, like HIF1α, DDB2 is also activated by ROS. We showed that ROS increases transcription of DDB2 mRNA, and that increase is related to activation of p38MAPK/JNK pathways, which activate the transcription factor AP1 [37]. Moreover, ROS increases binding of AP1 onto the DDB2 promoter. Inhibition of the p38MAPK/JNK causes loss of ROS-induced binding of AP1 to the DDB2 promoter, leading to inhibition of DDB2 expression by ROS [37]. Given both HIF1α and DDB2 are activated by ROS, we investigated whether these two proteins are functionally related. In this study, we reveal a novel role of DDB2 as a constitutive transcriptional repressor of HIF1α in HNSCC.

Results

Hypoxia increases expression of DDB2

We investigated DDB2 in HNSCC cells because of our recent finding that DDB2 is downregulated in the aggressive forms of HNSCC [38]. Moreover, we showed that the expression of DDB2 in mesenchymal type of HNSCC cells induces a change in morphology to epithelial-like, a MET-like change [38]. Since epithelial-to-mesenchymal transition occurs in hypoxic environment in tumors, we investigated the effects of hypoxia on DDB2. We observed significant upregulation of the DDB2 protein in HNSCC cells upon hypoxia treatments. For example, in SCC9 and SCC15 oral-SCC cells, during 72 h treatment in hypoxic chamber, there were significant increases in the protein levels of DDB2, compared with those in cells grown in normoxia, as judged by western blotting (Fig. 1b, c). However, no detectable upregulation of DDB2 protein was observed in hTERT-immortalized normal oral keratinocyte (HOK-TERT) cells (Fig. 1a).

Evidence for hypoxia-induced expression of DDB2 was observed also by immunofluorescence (IF). SCC15 cells grown on coverslips were subjected to hypoxia ($1\%O_2$), followed by IF assay for DDB2. As shown in Fig. 1e, culturing of SCC15 cells under hypoxic condition for 72 h caused a significant increase in the nuclear accumulation of DDB2. However, the IF-signal intensity of DDB2 in HOK-TERT cells remained unchanged after hypoxia treatment (Fig. 1d). Previously, we showed that ROS could increase the expression of DDB2 [37, 39]. Since hypoxia increases ROS-signaling pathways, we investigated whether the increase in DDB2 is related to ROS. We carried out hypoxia treatment in the presence of the anti-oxidant N-acetylcysteine (NAC) that inhibits ROS accumulation. Consistent with the idea, NAC inhibited hypoxia-induced increase in the levels of DDB2 (Fig. 1f).

DDB2 inhibits HIF1α

Next, we investigated whether DDB2 has any effect on HIF1α in HNSCC cells. We used two HNSCC cell lines, SCC9 cells expressing low DDB2, and SCC15 cells that express DDB2 at high level. For the SCC9 cells, we used stable pools of T7-epitope tagged DDB2 overexpressing, SCC9:T7-DDB2 and its vector control counterpart SCC9: B0 cells [6]. For the SCC15 cells, we used stable pools of control shRNA expressing (SCC15:sh-Cont) and DDB2-shRNA expressing (SCC15:shDDB2) cells [6]. Under normoxic growth condition in the DDB2 overexpressing SCC9:T7-DDB2 cells, there was a significant reduction in the level of HIF1α, whereas in SCC15:shDDB2 cells, there was significant upregulation of HIF1α as judged by western blot assay (Fig. 2a, e). The result was further confirmed by IF assay, in which we observed significant reduction of the nuclear staining of HIF1α in SCC9:T7-DDB2 cells following $CoCl_2$ treatment that mimics hypoxia (Fig. 2b). In contrast, clear increases in the immunostaining intensity of HIF1α was observed in SCC15:shDDB2 cells following depletion of DDB2 and cobalt chloride treatment (Fig. 2f). Furthermore, during hypoxic growth ($1\%O_2$) condition in shDDB2: SCC15 cells, a 2.5-fold increase in the HIF1α protein was observed in comparison to the control cells (Fig. 2g).

DDB2 does not alter the decay rate of HIF1α

Next, we investigated whether DDB2 regulates the levels of HIF1α by reducing the stability of HIF1α protein during hypoxia. HIF1α is readily degraded at normoxia with half-life of <5 min [40]. To determine whether DDB2 increases the decay rate of HIF1α, we treated cells with hypoxia-mimic cobalt chloride ($CoCl_2$, 300 μM) for four hours to block hydroxylation, then cycloheximide (CHX) was added to inhibit new protein synthesis, and cells were harvested at different time points. The cell-extracts were assayed for the HIF1α protein level. As shown in Fig. 2c, the HIF1α protein levels were significantly different in DDB2 overexpressing SCC9 cells as compared with control, however, the decay rates of HIF1α in the presence and absence of DDB2 overexpression were similar (Fig. 2d). Thus, while DDB2 reduces the protein levels of HIF1α, it has no apparent effect on the stability of HIF1α.

DDB2 directly represses transcription of *HIF1A* gene

RNA assays confirmed that HIF1α mRNA level was regulated by DDB2 (Fig. 3a, b). For example, HIF1α mRNA level was upregulated upon knockdown of DDB2 in SCC15 cells in comparison to the respective parental cells (Fig. 3a). Conversely, overexpression of DDB2 repressed the levels of HIF1α mRNA in SCC9 cells (Fig. 3b). HIF1α is primarily upregulated by stabilization during hypoxia and regulates multiple genes associated with cancer progression. Since, we observed an inverse co-relation between DDB2 and HIF1α mRNA expression under normoxic growth condition, we analyzed the regulation of both mRNA expressions during hypoxia in control SCC9:B0 and DDB2 overexpressing SCC9:T7-DDB2 cells. Interestingly, we observed repression of HIF1α mRNA in both cell types during hypoxic growth but increase in DDB2 mRNA expression (Fig. 3c). DDB2 had no significant effects on the expression of the HIF1α regulators, PHD2, and VHL (Fig. 3d, e).

DDB2 was shown to associate with specific DNA-element in the promoter region of its target genes, including *MnSOD, BCL2, NFKBIA, and NEDD4L* [32, 34, 36, 41]. To study whether DDB2 also associates with the HIF1A promoter, chromatin immunoprecipitation (ChIP) [42] assays were conducted using both SCC9:T7-DDB2 cells and SCC15 cells (Fig. 4, Supplementary Fig. S1A). Ten pairs of primers were designed to cover 5000 bp upstream of HIF1α transcription start site (Fig. 4a). For the SCC15 cells, ChIP of endogenous DDB2 recruitment to the *HIF1A* promoter was carried out with DDB2-antibody (DDB2-Ab) probing 5000 bp upstream of *HIF1A gene* (Fig. 4b). In DDB2 overexpressing SCC9:T7-DDB2 cells, the ChIP experiment was carried out with T7-antibody to determine the interaction of exogenous DDB2 with the HIF1A promoter (Supplementary Fig. S1A). The ChIP results demonstrated specific interactions of both endogenous and exogenous DDB2 with two consecutive chromatin fragments, P9 and P10 near the transcription start site (Fig. 4b, S1A). Interestingly, a putative DDB2-binding element *GCTTGCTGCC*, which is one nucleotide different from the one found in *BCL2* promoter and MNSOD [30, 34], is located in the chromatin fragment P10 (Fig. 4a). Previously, we showed that DDB2 epigenetically regulates *VEGF, ZEB1*, and *SNAIL* through interaction with the Suv39h1 histone methyltransferase mediated methylation of H3K9Me3 [33]. We performed ChIP experiments with H3K9Me3-antibody. In agreement with the previous report, we observed evidence for significant enrichment of histone H3K9Me3 in the P9 and P10 promoter fragment of *HIF1A*-promoter (Fig. 4c and Supplementary Fig. S1B). The H3K9Me3 ChIP-signals were much reduced with the SCC15:shDDB2 cells in comparison to that with the SCC15:sh-Cont cells (Fig. 4c). Moreover, we observed evidence for DDB2-dependent recruitment of the H3K9-methylase Suv39h1 onto the P9 and P10 promoter fragments of HIF1A (Fig. 4d). DDB2 interacts with EZH2, however, under the same conditions, no recruitment of EZH2 was observed (Supplementary Fig. S1C). These results suggest that DDB2 directly represses the expression of *HIF1A* by recruiting Suv39h1 onto the HIF1A promoter in HNSCC.

DDB2 regulates hypoxia-response genes in HNSCC

Next, we compared the mRNA levels of genes that are part of a 15-gene hypoxia classifier signature [43] in SCC9:B0 and SCC9:T7-DDB2 cells by real-time PCR (Fig. 5a). Clearly, the hypoxia-signature genes are expressed at much lower levels in DDB2 expressing cells (Fig. 5a). Several of these genes were shown also to be activated by HIF1α [44]. Co-expression of HIF1α rescued expression, to varied degrees, of 8 out of the 11 genes we assayed in SCC9:T7-DDB2 cells (Fig. 5b), indicating that DDB2 inhibits many of these genes via inhibition of HIF1α. However, it is unclear why expression of HIF1α failed to rescue lysyl oxidase (*LOX), NDRG1,HMOX1*, and *SERPINA1.* Among them, LOX and NDRG1 promoters contain DDB2-cognate element, and we observed evidence for interactions of DDB2 with those promoters (Supplementary Fig. S2). It is possible that some of the hypoxia-induced genes are directly regulated by DDB2, and that the DDB2 regulation is dominant over HIF1α induction. However, this will require further analyses of these promoters. Since these genes are induced by hypoxia, we investigated the induction of these genes in SCC9:B0 and SCC9:T7-DDB2 cells during hypoxic growth for 24 h or 48 h. We observed different induction levels for genes including *BNIP3, LOX, NDRG1, FAM162A, VIM, SLC2A1*, and *CAIX* during hypoxia, and for all these genes, expressions

were significantly subdued with overexpression of DDB2 as compared with the control parental cells (Fig. 5c).

Reduced expression of DDB2 coincides with increased expression HIF1α in advanced HNSCC

We previously reported the loss of DDB2 expression in high-grade colon tumors of both human and mice origin [33] and we recently observed lower expression of DDB2 in advanced stages of tongue SCCs and larynx SCCs [38]. In this study, we compared the expression of DDB2 and HIF1α in HNSCC tumor tissue microarrays that contained triplicate cores per cases including 22 cases of SCC (11 tongue SCC and 11 larynx SCC), six adjacent normal tissues (NAT), four normal tissues (tongue), and two normal larynx tissues. Duplicate TMAs were probed for HIF1α and DDB2. We observed higher expression of HIF1α at advanced stages of tongue SCCs (Fig. 6a) and larynx SCCs (Fig. 6b). In contrast, HIF1α expression was not detected in normal tongue and larynx tissues or cancer NAT in which DDB2 expression is abundant. Quantifications of DDB2 and HIF1α in the samples clearly indicated an opposite expression pattern (Fig. 6c, d). Moreover, Pearson correlation analyses (Fig. 6e) further indicated a negative correlation between the expressions of the two proteins, a result we predicted if DDB2 inhibits the expression of HIF1α.

Inhibition of DDB2 promotes SCC tumor growth and angiogenic marker expression in xenograft tumors

To investigate the effects of DDB2 expression on SCC tumor growth, we subcutaneously injected one million SCC9 cells or SCC9 cells expressing T7-DDB2 in the opposite flanks of same mouse. The SCC9 cells developed tumors that exhibited sustained growth with time. However, the SCC9:T7-DDB2 cells overexpressing DDB2 failed to support the tumor growth (Fig. 7b), providing a strong evidence to the notion that DDB2 is a potent suppressor of SCC. In a similar set up of experiments, we injected the SCC15 cells or SCC15 cells expressing DDB2-shRNA. The SCC15:sh-Control cells developed tumors, but did not exhibit sustained growth after few weeks. The DDB2-shRNA expressing SCC15:shDDB2 cells, on the other hand, developed tumor with sustained growth (Fig. 7a, and Supplementary Fig. S3A) with evidence for neovascularization (Supplementary Fig. S3A, lower panel). We compared the sections from the control SCC15-derived tumors with those from the DDB2-shRNA expressing SCC15-derived tumors, by immunohistochemistry (IHC) staining for Ki67, HIF1α, and the angiogenic markers CD31 and VEGF. Clearly, the DDB2-shRNA expressing tumors are highly proliferating with increased expression of Ki67 and HIF1α (Fig. 7c, d and Supplementary Fig. S3B). Moreover, as expected from increased HIF1α expression, the DDB2-shRNA expressing tumors also expressed the angiogenic markers CD31 and VEGF at higher levels compared with those derived from control SCC15 cells (Fig. 7c, d).

Discussion

The results presented in this report are significant in several ways. First, we show that DDB2 is a hypoxia-activated gene, and that DDB2 transcriptionally regulates the

expression of HIF1α in HNSCC, both in hypoxia and in normoxia. Moreover, DDB2 regulates the expression of hypoxia-signature genes. Loss of DDB2 enhances SCC tumor growth, coinciding with increased expression of HIF1α and the angiogenic markers. These observations suggest that DDB2 plays an important role in negatively regulating hypoxia-induced changes in HNSCC.

HNSCC is the sixth most common cancers of the world and yet has higher mortality rate with only 57% of patients are expected to survive in the next 5 years, which did not improve for last 20 years [45]. The high mortality rate has been linked to aggressive types of HNSCC that exhibit changes related to hypoxia [46]. Hypoxia is a common feature associated with majority of solid tumors due to uncontrolled proliferation and aberrant vasculature. In this report, we show that the NER factor DDB2, which is downregulated in high-grade HNSCC [38], constitutively represses HIF1α, a master transcriptional inducer of response to hypoxia. Moreover, we provide evidence that the expression of DDB2 has a significant effect on hypoxia responsive genes in HNSCC cells. The results presented here identify a novel transcriptional regulatory function of DDB2 that acts as suppressor of hypoxia by directly repressing HIF1α and hypoxia-mediated activation of transcriptional response triggered by HIF1α.

Exposure to hypoxia markedly upregulated DDB2 levels in SCC9 and SCC15 cells, independently of p53 since both of them carry mutations in p53 gene. The mechanism of this upregulation most likely involves ROS, as treatments with NAC blocked hypoxia-mediated increase in the levels of DDB2. ROS mediated induction of DDB2 was reported previously [37, 39]. ROS was suggested to be involved in the stabilization of HIF1α [42]. It was shown that a functional mitochondrial complex III is required for hypoxia-induced ROS production, and for HIF1α stabilization upon hypoxia [47].

Also, we provided evidence that DDB2 binds to a promoter-proximal region in the *HIF1A gene*. Interestingly, we observed the interaction of DDB2 with *HIF1A* chromatin at a region that also contains a DDB2-cognate element. (Fig. 4a). The DDB2-cognate element in the HIF1A promoter matches (90%) with the core sequence reported for DDB2 binding in the *MnSOD* and *BCL2* promoter [32, 34]. The epigenetic regulation of *HIF1A* promoter through histone mark H3K9Me3 by DDB2 and Suv39h1 is similar to what was reported for DDB2-mediated repression of EMT-regulatory genes, *VEGF, ZEB1*, and *SNAIL* [33].

The analysis of hypoxia responsive genes upon DDB2 overexpression revealed the regulation of genes that are emerging biomarkers for HNSCC [44, 48]. The genes that were downregulated by DDB2 closely related to genes that are not only upregulated in HNSCC but also have both, prognostic and predictive bearing on hypoxic modification. A group of these target genes including *CAIX* and *LOX* has a prognostic significance in other cancer types, as they have been investigated independently and their increased expression has been co-related with tumor hypoxia and poor prognosis [43, 44, 49–52]. LOX and CAIX are considered potential biomarkers for HNSCC and expression of these markers have been validated in specimens from clinical trials [53, 54]. CAIX was established as a functional mediator of hypoxia-induced stress response and contributes to several critical biological processes, including cell adhesion, survival, pH regulation, migration,

and invasion that helps to promote tumor progression and metastasis [55]. LOX is a copper dependent metallo-enzyme implicated in the metastasis of HNSCC by acting as an extracellular modulating protein that initiates cross-linking of collagens and elastin in ECM [56]. Other genes including THBS1 and BDNF were found to promote tumorigenesis and invasion in several human malignancies including oral and lung SCCs [57–62]. Markers like HMOX1 were associated with malignant progression of HNSCC [63]. Overall, among the 15-hypoxia-signature genes identified in HNSCC, we found many are regulated by DDB2 through a down regulation of HIF1α. That is consistent also with the inhibition of SCC tumor development by DDB2 in mouse xenografts.

In conclusion, DDB2 is a candidate regulator of *HIF1A* gene expression, and thus constitutively represses the expression of hypoxia-target genes in HNSCC. These observations add to the repertoire of tumor suppressor functions of DDB2. This observation reveals and hints at the possibility of using DDB2 as a cancer biomarker, which highlights its therapeutic value in hypoxic HNSCC.

Methods and materials

Cell culture

Oral squamous carcinoma cell lines, SCC9, and SCC15 were purchased from ATCC and cultured in 1:1 mixture of Dulbecco's modified eagle's medium and Ham's F12 with 10% FBS (Hyclone) supplemented with 200 μM L-glutamine, penicillin streptomycin 100 units, and 400 ng/ml hydrocortisone. Cells were cultured at 37°C in a humidified ambience containing 5% CO_2. Cell culture under 1% oxygen levels (hypoxia) was performed in a dedicated 37°C chamber monitored by a Thermo Scientific™ Heracell™ 240i Tri-Gas Incubator (Thermo Fisher Scientific, Waltham, MA) calibrated according to the manufacturer's instructions. Cells were cultured in normoxia (5%CO_2/21%O_2) for 24 h before transferring to the hypoxia chamber (1%O_2/5% CO_2) for hypoxic growth for the indicated period of time. Generation and characterization of the stable pools of T7-DDB2-expressing SCC9 cells (SCC9:T7-DDB2) and shDDB2 expressing SCC15 cells (SCC15:shDDB2) have been described before [38].

qRT-PCR analysis

mRNA expression was determined by qRT-PCR analysis following previously described method [38]. Briefly, total RNA was isolated using Trizol and 2 μg of total RNA was reverse transcribed into cDNA using M-MLV reverse transcriptase and Oligo dT primer. Authenticated PCR primers were used for the qRT-PCR assay using Ssoadvance SYBR kit on a CFX96 real-time PCR (Bio-Rad, Hercules, CA). Data analysis was performed using Bio-Rad CFX Manager software to determine Ct values and fold changes in expression by comparative Ct method. Primer sequences are included in the Supplementary information (Table S1). For the HIF1α rescue experiment as described in Fig. 5b, SCC9:T7-DDB2 cells were transfected with HIF1B cDNA (21101, addgene) using Lipofectamin 2000, Invitrogen. Forty-eight hours post transfection, total RNA was isolated using Trizol (Invitrogen), and analyzed by qRT-PCR for mRNA expression of the indicated genes.

Antibodies, western blot, and half-life assay

Antibodies used in the study were HIF1α-Ab (610958, BD Bio-Sciences); HIF1α-Ab (NB100–105, Novus Biologicals), HIF1α-Ab (ab51608, Abcam). DDB2-Ab (#5416, Cell Signaling), DDB2-Ab (Ab-77765, Abcam), and DDB2-Ab (sc-25368, Santa Cruz Biotechnology). HRP-conjugated secondary antibodies were from Santa Cruz Biotechnology. Cell lysates were made in RIPA buffer and western blot assays were performed following previously described method [38]. The half-life of HIF1α protein was determined using the CHX assay. Briefly, SCC9 cells were pretreated with $CoCl_2$ (300 μM) for 4 h followed by treatment with 50 μg/ml of CHX for indicated time period (0–60 min). Cell lysates were analyzed for the expression of DDB2, HIF1α, and β-actin. The normalized % residual HIF1α was plotted against the different time points to determine the half-life of HIF1α.

IF assay

IF experiments were performed using cells grown on coverslips as described previously [38]. For DDB2 immunostaining, cells were incubated overnight at 4°C with DDB2-Ab (SC-25368, Santa Cruz Biotechnology) or DDB2-Ab (Ab-77765, Abcam), and for HIF1α immunostaining, cells were incubated with HIF1α-Ab (NB100–105, Novus Biologicals). For hypoxia induction, cells were cultured in hypoxia chamber (1% O_2) for 48 h. Cells were incubated with anti-mouse secondary antibody Alexa Fluor 488 (Thermo Fisher Scientific) or anti-rabbit TRITC (Sigma) for 1 h at room temperature. Coverslips were mounted onto glass slides using Vectashield Antifade mounting media with DAPI (Vector Laboratories). Images were acquired using a Zeiss LSM 510 microscope using ×63 oil immersion objective.

Tissue microarrays

Paraffin-embedded tissue microarray slides containing human HNSCC tissues (HN811a; and HN242a) were obtained from US Biomax.Inc. Rockville, MD., and were subjected to IHC staining as described before [38]. The tissues were incubated overnight with the DDB2-Ab (Ab-77765, Abcam) or HIF1α-Ab (NB100–105, Novus Biologicals) diluted (1:100) in 3% normal serum. The tissues were incubated in biotinylated anti-rabbit antibody followed by ABC reagent using the Vectastain ABC kit PK-4001 as per the manufacturer's instruction. The enzymatic reaction was detected by adding DAB substrate, the sections were mounted in permount (Thermo Scientific). The slides were imaged using a Zeiss Axio Observer D1 inverted microscope.

Chromatin IP assay

SCC15 (parental), SCC15:sh-Cont, SCC15:shDDB2, and SCC9:T7-DDB2 cells were used for ChIP assay following a previously described method [64]. IP was carried out with T7-Ab from Novagen, DDB2-Ab (Ab-77765, Abcam) and H3K9Me3-Ab (Ab-8898, Abcam), SUV39H1-Ab (07–550, Millipore-Sigma), EZH2 (5246 S, Cell Signaling Technology) and rabbit immunoglobulin (IgG) from Santa Cruz Biotechnology. Reverse cross-linking was performed by overnight incubation at 65 °C in Tris-EDTA (TE) buffer containing 200 mM NaCl with 0.1 mg proteinase K/ml. DNA was extracted using a PCR purification kit

(Qiagen) and was amplified by qPCR alongside with 0.1% of the input chromatin used for IP. Promoter-specific primer sequences of human HIF1B, NDRG1, and LOX are listed in the Supplementary Table S2.

Animal studies

Athymic nude mice (NU/J 002019) were procured from the Jackson Laboratory for xenograft experiment. The animals were housed in pathogen free condition under 12 h of light and dark photoperiod with controlled humidity and temperature. Animal care and experimentation were preapproved by the UIC Institutional Animal Care and Use Committee. Six-week-old nude mice, three for each sets of experiments were injected subcutaneously with 1×10^6 cells in Matrigel either with SCC9:B0 (left flank) and SCC9:T7-DDB2 (right flank) or SCC15-sh-Control (left flank) and SCC15-shDDB2 (right flank) under aseptic condition. Tumor growth was observed for six weeks and the growth readings were taken once in every week. The mice were euthanized, and tumors were harvested for immunohistological studies.

Immunohistochemistry (IHC)

IHC staining of the xenograft tumor sections was performed using the standard procedure. Antigen retrieval was done using the citrate buffer followed by blocking with appropriate serum for an hour at room temperature. Overnight incubation with primary antibodies, DDB2-Ab (Ab-77765, Abcam), HIF1B-Ab (Ab-2185, Abcam), CD31-Ab (Ab-7388, Abcam), VEGF-Ab (Ab-46154, Abcam), and Ki67 (Ab-16667, Abcam) were done at 4 °C. An additional blocking step was performed using an avidin/biotin Vectastain kit following the manufacturer's protocol. Visualization was done using DAB and counterstain using hematoxylin (Polyscientific), sections were then analyzed under brightfield microscope (Lieca LAS-X). All reagents used are from Vector Labs.

Quantification and statistical analysis

Signal intensity of protein bands from western blots were quantified using Fiji version of ImageJ software. Intensity units were quantified from optical density as percent mean intensity using a formula OD = log (max intensity/mean intensity). Statistical analyses for difference between experimental groups (<2) were performed with GraphPad Prism software by using Student's unpaired *t* test. Statistical differences between more than two experimental groups were analyzed using one-way ANOVA with Tukey's post-hoc analysis for multiple comparisons. The data are expressed as means ± SD from three technical replicates and from three independent experiments as indicated in the figure legends. A value of $*P < 0.05$ was considered significant whereas a value of less than $**P < 0.01$ and $***P < 0.001$ was considered highly significant.

Supplementary Material

Refer to Web version on PubMed Central for supplementary material.

Acknowledgements

We thank members of PR and SB Laboratory for helpful guidance during this study. We especially thank Caius Coretchi for his technical assistance as summer research student in the College of Dentistry.

Funding

This work was supported by the grants from National Cancer Institute (NCI) to SB (R03CA227308) and the multi-PI grant from the National Cancer Institute (NCI) to PR and SB (R01CA156164).

References

1. Simon MC, Keith B. The role of oxygen availability in embryonic development and stem cell function. Nat Rev Mol Cell Biol. 2008;9:285–96. [PubMed: 18285802]
2. Semenza GL. Hypoxia-inducible factor 1: oxygen homeostasis and disease pathophysiology. Trends Mol Med. 2001;7:345–50. [PubMed: 11516994]
3. Iyer NV, Kotch LE, Agani F, Leung SW, Laughner E, Wenger RH, et al. Cellular and developmental control of O_2 homeostasis by hypoxia-inducible factor 1 alpha. Genes Dev. 1998;12:149–62. [PubMed: 9436976]
4. Vaupel P, Briest S, Hockel M. Hypoxia in breast cancer: pathogenesis, characterization and biological/therapeutic implications. Wien Med Wochenschr. 2002;152:334–42. [PubMed: 12168517]
5. Vaupel P, Thews O, Hoeckel M. Treatment resistance of solid tumors: role of hypoxia and anemia. Med Oncol. 2001;18:243–59. [PubMed: 11918451]
6. Nowrousian MR. (Editor) Recombinant Human Erythropoietin(rhEPO) in clinical oncology: Scientific and clinical aspects of anemia in cancer. 2nd edition, Springer Wlen New York; 2008.
7. Vaupel P, Kelleher DK, Hockel M. Oxygen status of malignant tumors: pathogenesis of hypoxia and significance for tumor therapy. Semin Oncol. 2001;28:29–35.
8. Keith B, Simon MC. Hypoxia-inducible factors, stem cells, and cancer. Cell. 2007;129:465–72. [PubMed: 17482542]
9. Koumenis C, Hammond E, Giaccia AJ. Tumor microenvironment and cellular stress: signaling, metabolism, imaging, and therapeutic targets. Preface. Adv Exp Med Biol 2014;772:v–viii. [PubMed: 24765667]
10. Sui H, Zhu L, Deng W, Li Q. Epithelial-mesenchymal transition and drug resistance: role, molecular mechanisms, and therapeutic strategies. Oncol Res Treat. 2014;37:584–9. [PubMed: 25342509]
11. Iyer AK, Singh A, Ganta S, Amiji MM. Role of integrated cancer nanomedicine in overcoming drug resistance. Adv drug Deliv Rev. 2013;65:1784–802. [PubMed: 23880506]
12. Wang GL, Jiang BH, Rue EA, Semenza GL. Hypoxia-inducible factor 1 is a basic-helix-loop-helix-PAS heterodimer regulated by cellular O_2 tension. Proc Natl Acad Sci USA. 1995;92:5510–4. [PubMed: 7539918]
13. Berra E, Richard DE, Gothie E, Pouyssegur J. HIF-1-dependent transcriptional activity is required for oxygen-mediated HIF-1alpha degradation. FEBS Lett. 2001;491:85–90. [PubMed: 11226425]
14. Radisky DC, Levy DD, Littlepage LE, Liu H, Nelson CM, Fata JE, et al. Rac1b and reactive oxygen species mediate MMP-3-induced EMT and genomic instability. Nature. 2005;436:123–7. [PubMed: 16001073]
15. Waypa GB, Smith KA, Schumacker PT. O2 sensing, mitochondria and ROS signaling: the fog is lifting. Mol Asp Med. 2016;47–48:76–89.
16. Chandel NS, Maltepe E, Goldwasser E, Mathieu CE, Simon MC, Schumacker PT. Mitochondrial reactive oxygen species trigger hypoxia-induced transcription. Proc Natl Acad Sci USA. 1998;95:11715–20. [PubMed: 9751731]
17. Pouyssegur J, Dayan F, Mazure NM. Hypoxia signalling in cancer and approaches to enforce tumour regression. Nature. 2006;441: 437–43. [PubMed: 16724055]

18. Dames SA, Martinez-Yamout M, De Guzman RN, Dyson HJ, Wright PE. Structural basis for Hif-1 alpha /CBP recognition in the cellular hypoxic response. Proc Natl Acad Sci USA. 2002;99:5271–6. [PubMed: 11959977]
19. Cam H, Easton JB, High A, Houghton PJ. mTORC1 signaling under hypoxic conditions is controlled by ATM-dependent phosphorylation of HIF-1alpha. Mol Cell. 2010;40:509–20. [PubMed: 21095582]
20. Lim JH, Lee YM, Chun YS, Chen J, Kim JE, Park JW. Sirtu in 1 modulates cellular responses to hypoxia by deacetylating hypoxia-inducible factor 1alpha. Mol Cell. 2010;38:864–78. [PubMed: 20620956]
21. Yoo YG, Kong G, Lee MO. Metastasis-associated protein 1 enhances stability of hypoxia-inducible factor-1alpha protein by recruiting histone deacetylase 1. EMBO J. 2006;25:1231–41. [PubMed: 16511565]
22. Cheng J, Kang X, Zhang S, Yeh ET. SUMO-specific protease 1 is essential for stabilization of HIF1Alpha during hypoxia. Cell. 2007;131:584–95. [PubMed: 17981124]
23. Bae SH, Jeong JW, Park JA, Kim SH, Bae MK, Choi SJ, et al. Sumoylation increases HIF-1alpha stability and its transcriptional activity. Biochem Biophys Res Commun. 2004;324:394–400. [PubMed: 15465032]
24. Li F, Sonveaux P, Rabbani ZN, Liu S, Yan B, Huang Q, et al. Regulation of HIF-1alpha stability through S-nitrosylation. Mol Cell. 2007;26:63–74. [PubMed: 17434127]
25. Ryu JH, Li SH, Park HS, Park JW, Lee B, Chun YS. Hypoxia-inducible factor alpha subunit stabilization by NEDD8 conjugation is reactive oxygen species-dependent. J Biol Chem. 2011;286:6963–70. [PubMed: 21193393]
26. Belaiba RS, Bonello S, Zahringer C, Schmidt S, Hess J, Kietzmann T, et al. Hypoxia up-regulates hypoxia-inducible factor-1alpha transcription by involving phosphatidylinositol 3-kinase and nuclear factor kappaB in pulmonary artery smooth muscle cells. Mol Biol Cell. 2007;18:4691–7. [PubMed: 17898080]
27. Rius J, Guma M, Schachtrup C, Akassoglou K, Zinkernagel AS, Nizet V, et al. NF-kappaB links innate immunity to the hypoxic response through transcriptional regulation of HIF-1alpha. Nature. 2008;453:807–11. [PubMed: 18432192]
28. Stoyanova T, Roy N, Kopanja D, Raychaudhuri P, Bagchi S. DDB2 (damaged-DNA binding protein 2) in nucleotide excision repair and DNA damage response. Cell Cycle. 2009;8:4067–71. [PubMed: 19923893]
29. Wittschieben BO, Iwai S, Wood RD. DDB1-DDB2 (xeroderma pigmentosum group E) protein complex recognizes a cyclobutane pyrimidine dimer, mismatches, apurinic/apyrimidinic sites, and compound lesions in DNA. J Biol Chem. 2005;280:39982–9. [PubMed: 16223728]
30. Wittschieben BO, Wood RD. DDB complexities. DNA repair. 2003;2:1065–9. [PubMed: 12967661]
31. Stoyanova T, Roy N, Bhattacharjee S, Kopanja D, Valli T, Bagchi S, et al. p21 cooperates with DDB2 protein in suppression of ultraviolet ray-induced skin malignancies. J Biol Chem. 2012;287:3019–28. [PubMed: 22167187]
32. Minig V, Kattan Z, van Beeumen J, Brunner E, Becuwe P. Identification of DDB2 protein as a transcriptional regulator of constitutive SOD2 gene expression in human breast cancer cells. J Biol Chem. 2009;284:14165–76. [PubMed: 19339246]
33. Roy N, Bommi PV, Bhat UG, Bhattacharjee S, Elangovan I, Li J, et al. DDB2 suppresses epithelial-to-mesenchymal transition in colon cancer. Cancer Res. 2013;73:3771–82. [PubMed: 23610444]
34. Zhao R, Han C, Eisenhauer E, Kroger J, Zhao W, Yu J, et al. DNA damage-binding complex recruits HDAC1 to repress Bcl-2 transcription in human ovarian cancer cells. Mol Cancer Res. 2014;12:370–80. [PubMed: 24249678]
35. Han C, Zhao R, Liu X, Srivastava A, Gong L, Mao H, et al. DDB2 suppresses tumorigenicity by limiting the cancer stem cell population in ovarian cancer. Mol Cancer Res. 2014;12:784–94. [PubMed: 24574518]

36. Zhao R, Cui T, Han C, Zhang X, He J, Srivastava AK, et al. .DDB2 modulates TGF-beta signal transduction in human ovarian cancer cells by downregulating NEDD4L. Nucleic Acids Res. 2015;43:7838–49. [PubMed: 26130719]
37. Roy N, Elangovan I, Kopanja D, Bagchi S, Raychaudhuri P. Tumor regression by phenethyl isothiocyanate involves DDB2. Cancer Biol Ther. 2013;14:108–16. [PubMed: 23114715]
38. Bommi PV, Ravindran S, Raychaudhuri P, Bagchi S. DDB2 regulates epithelial-to-mesenchymal transition (EMT) in oral/head and neck squamous cell carcinoma. Oncotarget. 2018;9: 34708–18. [PubMed: 30410671]
39. Roy N, Bagchi S, Raychaudhuri P. Damaged DNA binding protein 2 in reactive oxygen species (ROS) regulation and premature senescence. Int J Mol Sci. 2012;13:11012–26. [PubMed: 23109835]
40. Semenza GL. Hypoxia, clonal selection, and the role of HIF-1 in tumor progression. Crit Rev Biochem Mol Biol. 2000;35:71–103. [PubMed: 10821478]
41. Ennen M, Klotz R, Touche N, Pinel S, Barbieux C, Besancenot V, et al. DDB2: a novel regulator of NF-kappaB and breast tumor invasion. Cancer Res. 2013;73:5040–52. [PubMed: 23774208]
42. Cheung KJ, Padmanaban V, Silvestri V, Schipper K, Cohen JD, Fairchild AN, et al. Polyclonal breast cancer metastases arise from collective dissemination of keratin 14-expressing tumor cell clusters. Proc Natl Acad Sci USA. 2016;113:E854–E863. [PubMed: 26831077]
43. Sorensen BS, Knudsen A, Wittrup CF, Nielsen S, Aggerholm-Pedersen N, Busk M, et al. The usability of a 15-gene hypoxia classifier as a universal hypoxia profile in various cancer cell types. Radiother Oncol. 2015;116:346–51. [PubMed: 26169282]
44. Toustrup K, Sorensen BS, Metwally MA, Tramm T, Mortensen LS, Overgaard J, et al. Validation of a 15-gene hypoxia classifier in head and neck cancer for prospective use in clinical trials. Acta Oncol. 2016;55:1091–8. [PubMed: 27161763]
45. Parkin DM, Bray F, Ferlay J, Pisani P. Global cancer statistics,2002. CA Cancer J Clin. 2005;55:74–108. [PubMed: 15761078]
46. Brizel DM, Sibley GS, Prosnitz LR, Scher RL, Dewhirst MW. Tumor hypoxia adversely affects the prognosis of carcinoma of the head and neck. Int J Radiat Oncol Biol Phys. 1997;38:285–9. [PubMed: 9226314]
47. Guzy RD, Hoyos B, Robin E, Chen H, Liu L, Mansfield KD, et al. Mitochondrial complex III is required for hypoxia-induced ROS production and cellular oxygen sensing. Cell Metab. 2005;1:401–8. [PubMed: 16054089]
48. Toustrup K, Sorensen BS, Nordsmark M, Busk M, Wiuf C, Alsner J, et al. Development of a hypoxia gene expression classifier with predictive impact for hypoxic modification of radiotherapy in head and neck cancer. Cancer Res. 2011;71:5923–31. [PubMed: 21846821]
49. Hoskin PJ, Sibtain A, Daley FM, Wilson GD. GLUT1 and CAIX as intrinsic markers of hypoxia in bladder cancer: relationship with vascularity and proliferation as predictors of outcome of ARCON. Br J Cancer. 2003;89:1290–7. [PubMed: 14520462]
50. Overgaard J, Eriksen JG, Nordsmark M, Alsner J, Horsman MR, Danish H, et al. Plasma osteopontin, hypoxia, and response to the hypoxia sensitiser nimorazole in radiotherapy of head and neck cancer: results from the DAHANCA 5 randomised double-blind placebo-controlled trial. Lancet Oncol. 2005;6:757–64. [PubMed: 16198981]
51. Wykoff CC, Beasley NJ, Watson PH, Turner KJ, Pastorek J, Sibtain A, et al. Hypoxia-inducible expression of tumor-associated carbonic anhydrases. Cancer Res. 2000;60:7075–83. [PubMed: 11156414]
52. Albinger-Hegyi A, Stoeckli SJ, Schmid S, Storz M, Iotzova G, Probst-Hensch NM, et al. Lysyl oxidase expression is an independent marker of prognosis and a predictor of lymph node metastasis in oral and oropharyngeal squamous cell carcinoma (OSCC). Int J cancer. 2010;126:2653–62. [PubMed: 19816945]
53. Le QT, Harris J, Magliocco AM, Kong CS, Diaz R, Shin B, et al. Validation of lysyl oxidase as a prognostic marker for metastasis and survival in head and neck squamous cell carcinoma: radiation therapy oncology group trial 90–03. J Clin Oncol. 2009;27: 4281–6. [PubMed: 19667273]

54. Perez-Sayans M, Supuran CT, Pastorekova S, Suarez-Penaranda JM, Pilar GD, Barros-Angueira F, et al. The role of carbonic anhydrase IX in hypoxia control in OSCC. J Oral Pathol Med. 2013;42:1–8. [PubMed: 22417164]

55. McDonald PC, Dedhar S. Carbonic anhydrase IX (CAIX) as a mediator of hypoxia-induced stress response in cancer cells. Subcell Biochem. 2014;75:255–69. [PubMed: 24146383]

56. Erler JT, Bennewith KL, Nicolau M, Dornhofer N, Kong C, Le QT, et al. Lysyl oxidase is essential for hypoxia-induced metastasis. Nature. 2006;440:1222–6. [PubMed: 16642001]

57. Hayashido Y, Nakashima M, Urabe K, Yoshioka H, Yoshioka Y, Hamana T, et al. Role of stromal thrombospondin-1 in motility and proteolytic activity of oral squamous cell carcinoma cells. Int J Mol Med. 2003;12:447–52. [PubMed: 12964017]

58. Horiguchi H, Yamagata S, Rong Qian Z, Kagawa S, Sakashita N. Thrombospondin-1 is highly expressed in desmoplastic components of invasive ductal carcinoma of the breast and associated with lymph node metastasis. J Med Investig. 2013;60:91–96. [PubMed: 23614916]

59. Jayachandran A, Anaka M, Prithviraj P, Hudson C, McKeown SJ, Lo PH, et al. Thrombospondin 1 promotes an aggressive phenotype through epithelial-to-mesenchymal transition in human melanoma. Oncotarget. 2014;5:5782–97. [PubMed: 25051363]

60. Pal SK, Nguyen CT, Morita KI, Miki Y, Kayamori K, Yamaguchi A, et al. THBS1 is induced by TGFB1 in the cancer stroma and promotes invasion of oral squamous cell carcinoma. J Oral Pathol Med. 2016;45:730–9. [PubMed: 26850833]

61. Zhang SY, Hui LP, Li CY, Gao J, Cui ZS, Qiu XS. More expression of BDNF associates with lung squamous cell carcinoma and is critical to the proliferation and invasion of lung cancer cells. BMC Cancer. 2016;16:171. [PubMed: 26926340]

62. Firlej V, Mathieu JR, Gilbert C, Lemonnier L, Nakhle J, Gallou-Kabani C, et al. Thrombospondin-1 triggers cell migration and development of advanced prostate tumors. Cancer Res. 2011;71:7649–58. [PubMed: 22037878]

63. Gandini NA, Fermento ME, Salomon DG, Blasco J, Patel V, Gutkind JS, et al. Nuclear localization of heme oxygenase-1 is associated with tumor progression of head and neck squamous cell carcinomas. Exp Mol Pathol. 2012;93:237–45. [PubMed: 22580187]

64. Huang S, Fantini D, Merrill BJ, Bagchi S, Guzman G, Raychaudhuri P. DDB2 is a novel regulator of wnt signaling in colon cancer. Cancer Res. 2017;77:6562–75. [PubMed: 29021137]

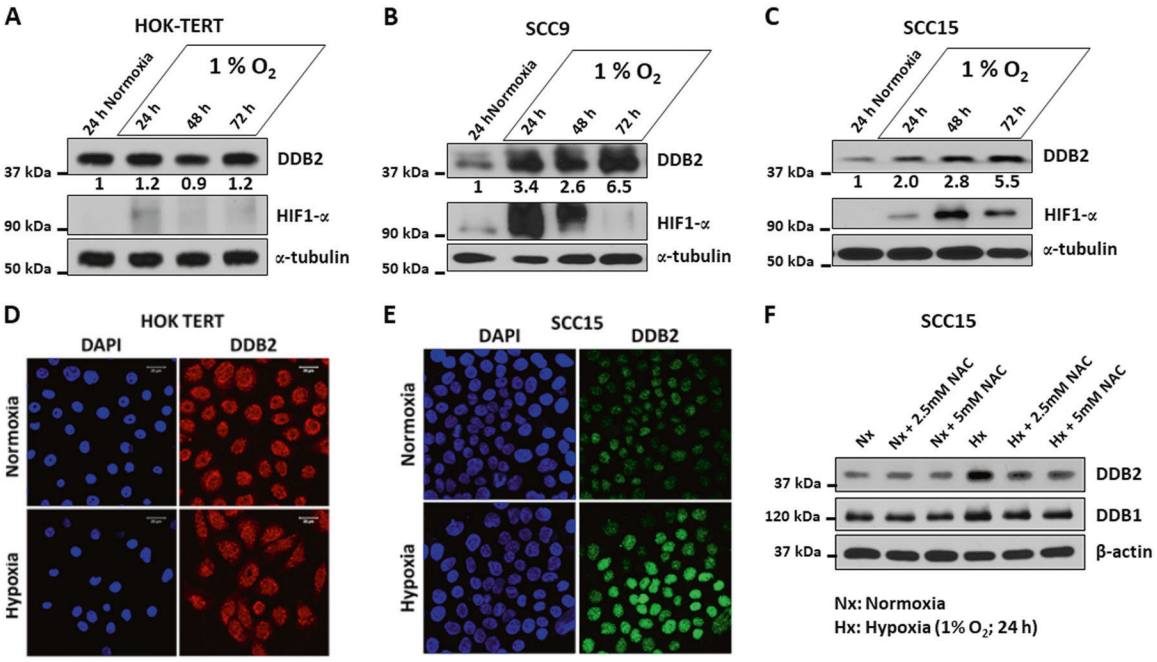

Fig. 1.

DDB2 expression is increased in response to hypoxia. The hTERT-immortalized human oral keratinocytes (HOK-TERT) (**a**) and the oral-SCC cell lines, SCC9 (**b**) and SCC15 (**c**) were cultured under normoxic (21% O_2) and hypoxic (1% O_2) condition for the indicated time. Cell lysates were subjected to western blot analysis using DDB2-Ab, HIF1α-Ab or tubulin-Ab (loading control). Relative expression of DDB2 during hypoxia were normalized against normoxia, quantitation was conducted by densitometric analysis using ImageJ software. **d**, **e** Representative images of DDB2 immunostaining after cells were grown in normoxia or hypoxia (1% O_2 for 72 h). **d** HOK-TERT cells were subjected to immunocytochemical staining with polyclonal DDB2-Ab followed by fluorophore conjugated secondary antibody (anti-Rabbit-TRITC). **e** SCC15 cells were stained with DDB2-Ab followed by secondary antibody (anti-mouse-Alexa Fluor 488). The cell nuclei were counterstained with DAPI (Blue). **f** ROS regulates DDB2 expression during hypoxia. SCC15 cells were grown in normoxia and hypoxia with or without ROS-inhibitor NAC (N-acetyl cysteine) at indicated concentration for 24 h. Lysates were subjected to western blot analysis using antibodies against DDB2, DDB1, or β-actin (loading control).

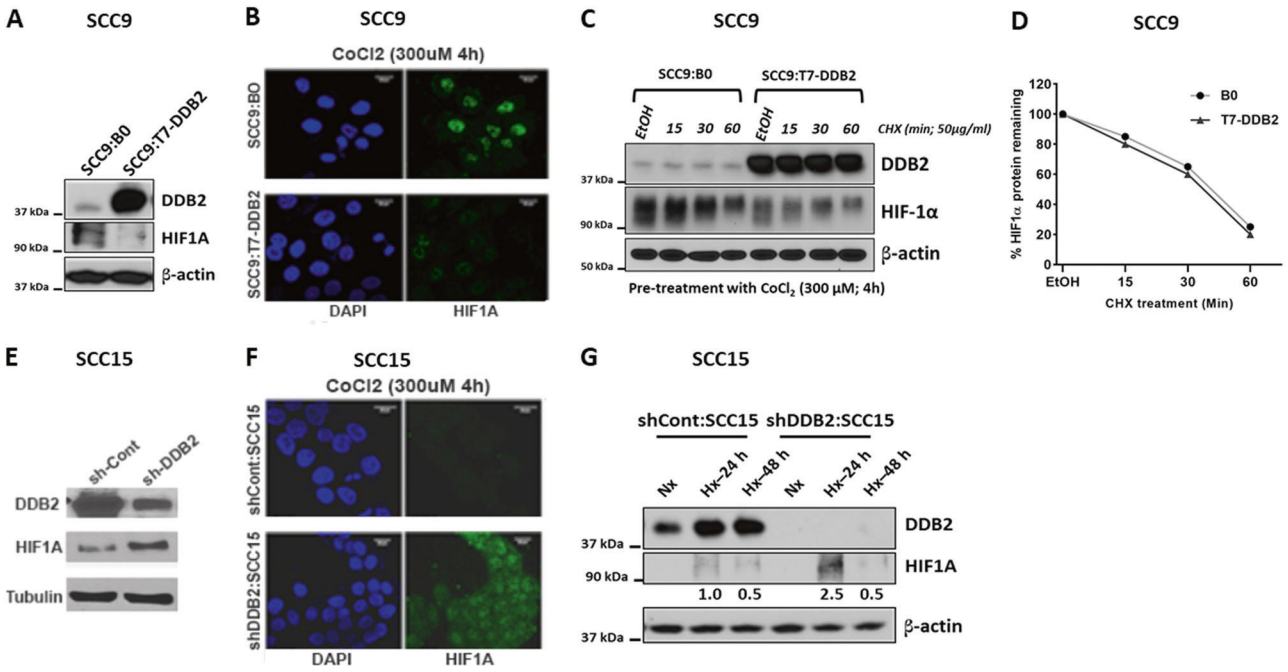

Fig. 2.

DDB2 represses HIF1α protein both in normoxia and in hypoxia but does not alter its decay rate. DDB2 inhibits expression of HIF1α protein. **a** Total cell lysates from stable pools of SCC9:B0 or SCC9:T7-DDB2 were subjected to western blot analysis and probed with DDB2-Ab, HIF1α-Ab or β-actin-Ab. **b** SCC9:B0 and SCC9:T7-DDB2 cells treated with $COCl_2$ were subjected to immunocytochemical staining for HIF1α (Green) and imaged with confocal microscopy, the cell nuclei were counterstained with DAPI (Blue). **c** HIF1α protein stability did not change significantly upon DDB2 overexpression. SCC9:B0 and SCC9:T7-DDB2 cells pretreated with $COCl_2$ were incubated with cycloheximide (CHX; 50 μg/ml) for the indicated time. Cell lysates were probed with the indicated antibodies using western blot assay. **d** HIF1α protein levels were plotted as percent (%)HIF1α remaining compared with 0 h (EtOH) of CHX treatment. Densitometry and quantitative analysis were performed using ImageJ software, **e** Knockdown of DDB2 in SCC15 cells elevates HIF1α level during normoxic growth. Cell lysates from stable pools of SCC15:sh-Cont or SCC15:shDDB2 cells were probed with DDB2-Ab, HIF1α-Ab or tubulin-Ab using western blot assay. **f** SCC15:sh-Cont and SCC15: shDDB2 cells treated with $COCl_2$ were stained for HIF1α (Green) and imaged with confocal microscopy, the cell nuclei were counterstained with DAPI (Blue). **g** HIF1α levels are elevated in SCC15:shDDB2 during hypoxia in comparison to SCC15:sh-Cont. SCC15:sh-Cont and SCC15:shDDB2 cells were cultured under normoxic or hypoxic (1% O_2) condition for the indicated time. Cell lysates were probed with DDB2-Ab, HIF1α-Ab. or β-actin-Ab (loading control) using western blot assay.

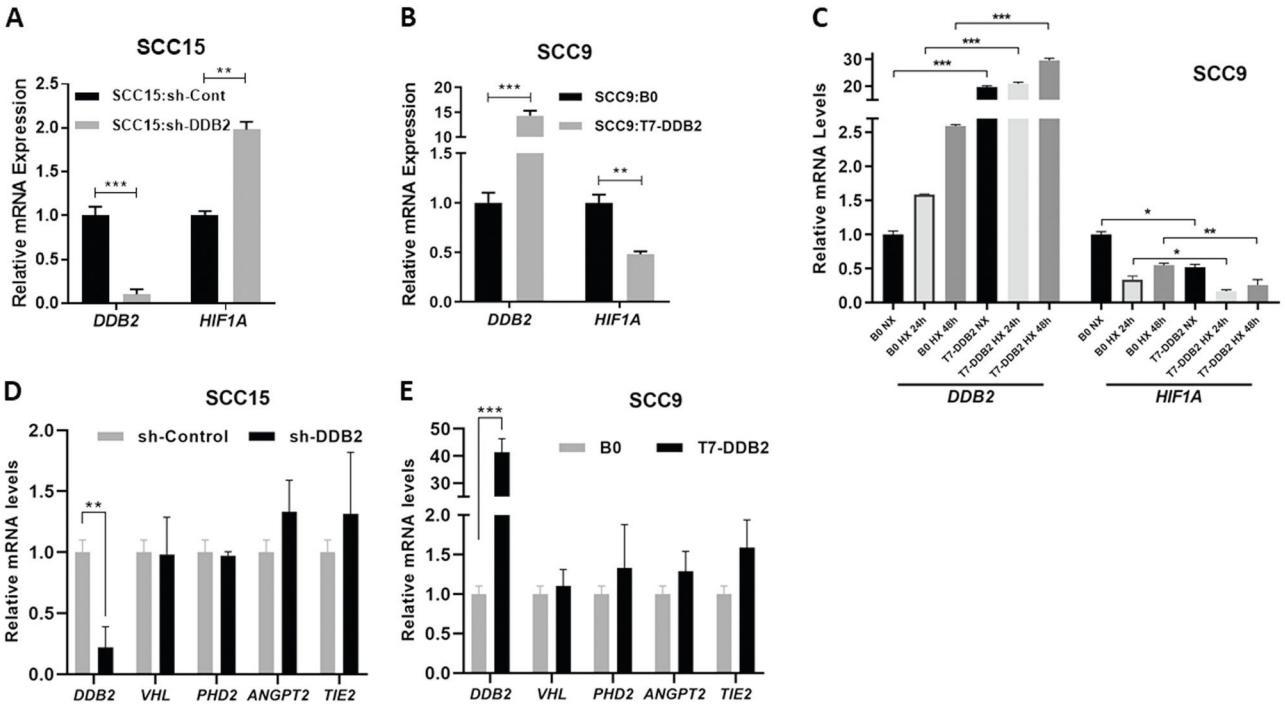

Fig. 3.

DDB2 regulates HIF1α mRNA level. DDB2 represses HIF1α mRNA expression both in normoxia and hypoxia. Relative mRNA expression of DDB2 and HIF1α in SCC15:sh-Cont and SCC15: shDDB2 cells (**a**) or DDB2 overexpressing SCC9:T7-DDB2 and control SCC9:B0 cells (**b**) are shown. **c** SCC9:B0 and SCC9:T7-DDB2 cells were cultured in normoxia (NX) or hypoxia (HX) (1% O_2) for 24 h or 48 h. Relative expression of DDB2- and HIF1α-mRNA were analyzed by qRT-PCR. DDB2 does not repress the HIF1α-regulatory genes *VHL* and *PHD2* and angiogenesis genes *ANGPT2* or *TIE2*. Relative mRNA expression of *VHL, PHD2, ANGPT2*, and *TIE2* in SCC15:sh-Cont and SCC15:shDDB2 cells (**d**) or SCC9:B0 and SCC9:T7-DDB2 cells (**e**) are shown. Data are expressed as fold changes between SCC9:T7-DDB2 and SCC9:B0 cells. Error bars, ± SD. $*P < 0.05$, $**P < 0.01$, $***P < 0.001$ by the Student's *t* test (unpaired).

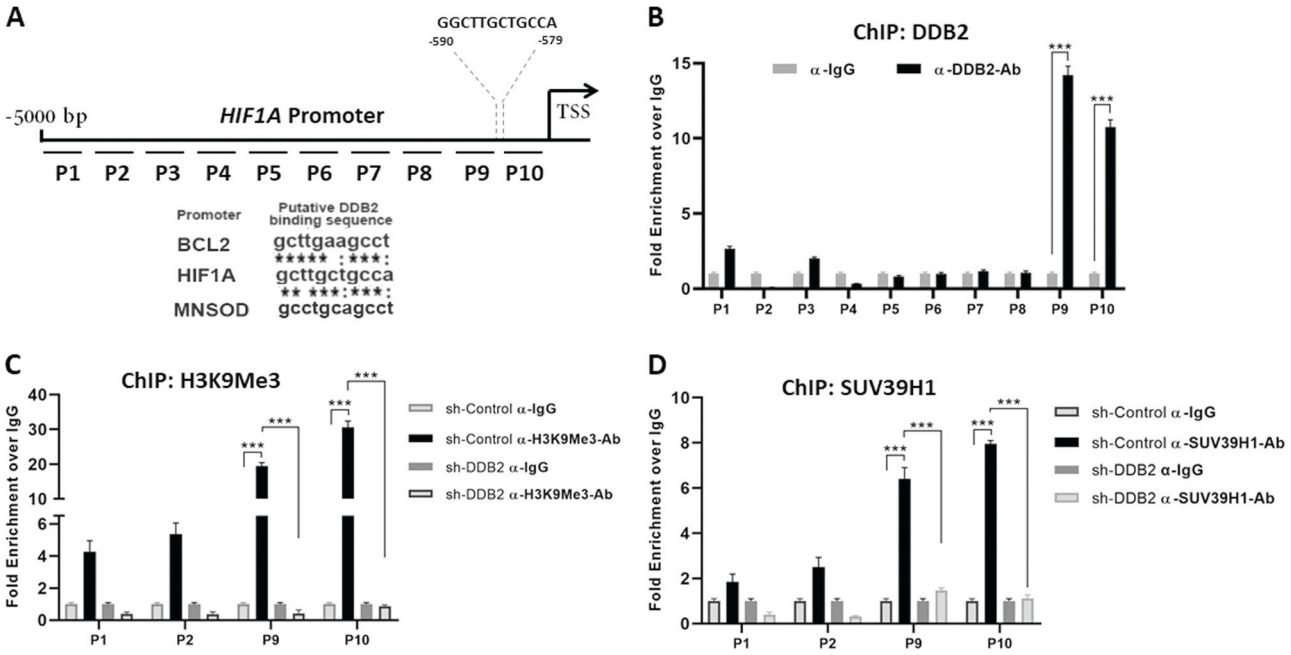

Fig. 4.

DDB2 binds to the promoter region of the HIF1A gene and promotes H3K9 trimethylation around the binding site. **a** The schematic diagram of human HIF1A gene promoter with the truncated lines representing the primer sets P1–P10 used for the ChIP-analysis. The putative DDB2-binding site at 590 bp upstream of transcription start site (TSS) is shown. The lower panel shows the sequence alignment of putative DDB2-binding site at −590 of HIF1A gene with the published DDB2-binding sites of MnSOD and BCL2 gene and significant homology. **b** Parental SCC15 cells were subjected to ChIP assay using DDB2-Ab and isotype matched control IgG as described in materials and methods. The relative fold enrichment was quantified by normalization to input first, then normalized to IgG, which is set at one. Furthermore, comparative quantitative ChIP assays in SCC15:sh-Control and SCC15:shDDB2 were performed using H3K9Me3-Ab (trimethylated histone H3 K9-antibody) (**c**) and Suv39h1-Ab (**d**). Chip-data using HIF1B promoter fragments P1, P2, P9, and P10 are shown. Data are expressed as ± SD. One-way ANOVA, $*P < 0.05$, $**P < 0.01$ wherever indicated.

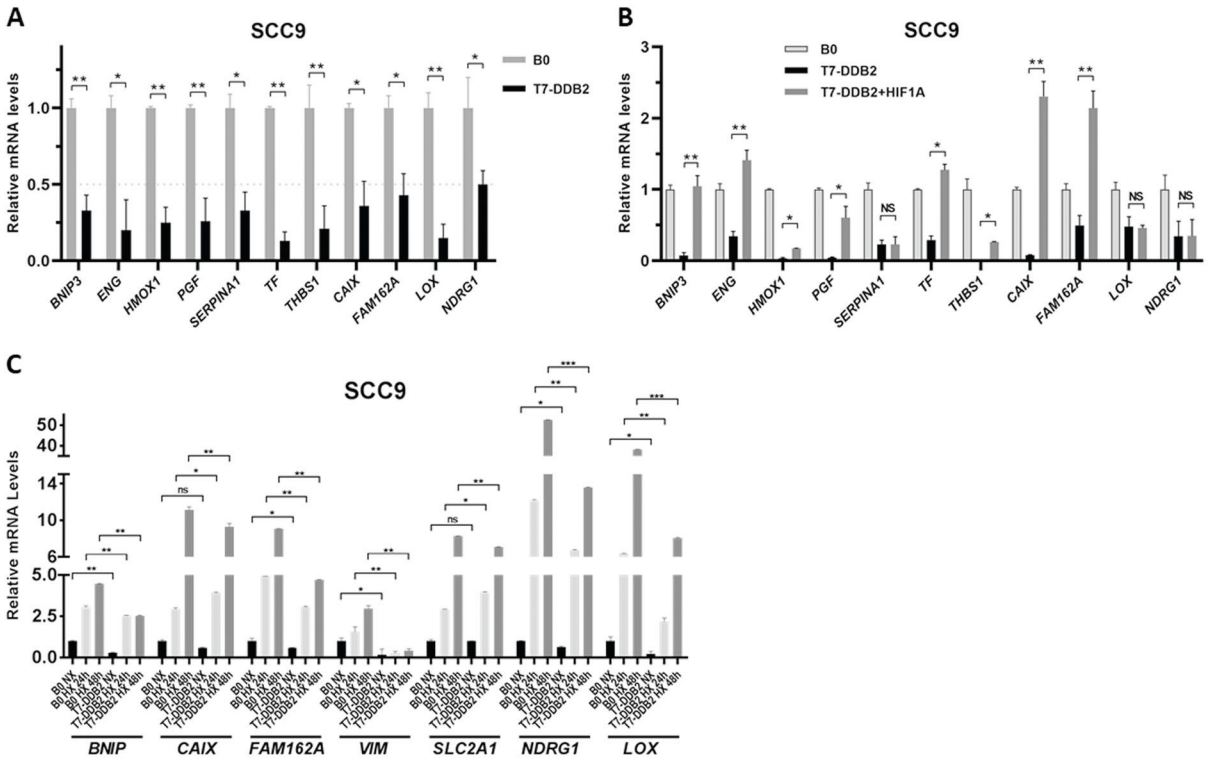

Fig. 5.

DDB2 represses expression of key hypoxia-response genes. a Total RNA isolated from SCC9:B0 and SCC9:T7-DDB2 cells were analyzed by qRT-PCR for mRNA expression of key hypoxia-signature genes that are used as biomarkers in HNSCC. **b** Rescue of the DDB2-dependent transcriptional repression of the hypoxia-signature genes upon overexpression of HIF1α in SCC9:T7-DDB2 cells is shown. **c** DDB2 represses the expression of key hypoxia-signature genes both in normoxia and hypoxia. Control SCC9:B0 and DDB2 overexpressing SCC9:T7-DDB2 cells were cultured in normoxia (NX) or hypoxia (HX) (1% O_2) for 24 h or 48 h. Relative expression levels of the indicated genes were analyzed by qRT-PCR. Data are expressed as fold changes between SCC9:T7-DDB2 and control SCC9:B0. Data are shown as ± SD. One-way ANOVA, $*P < 0.05$, $**P < 0.01$.

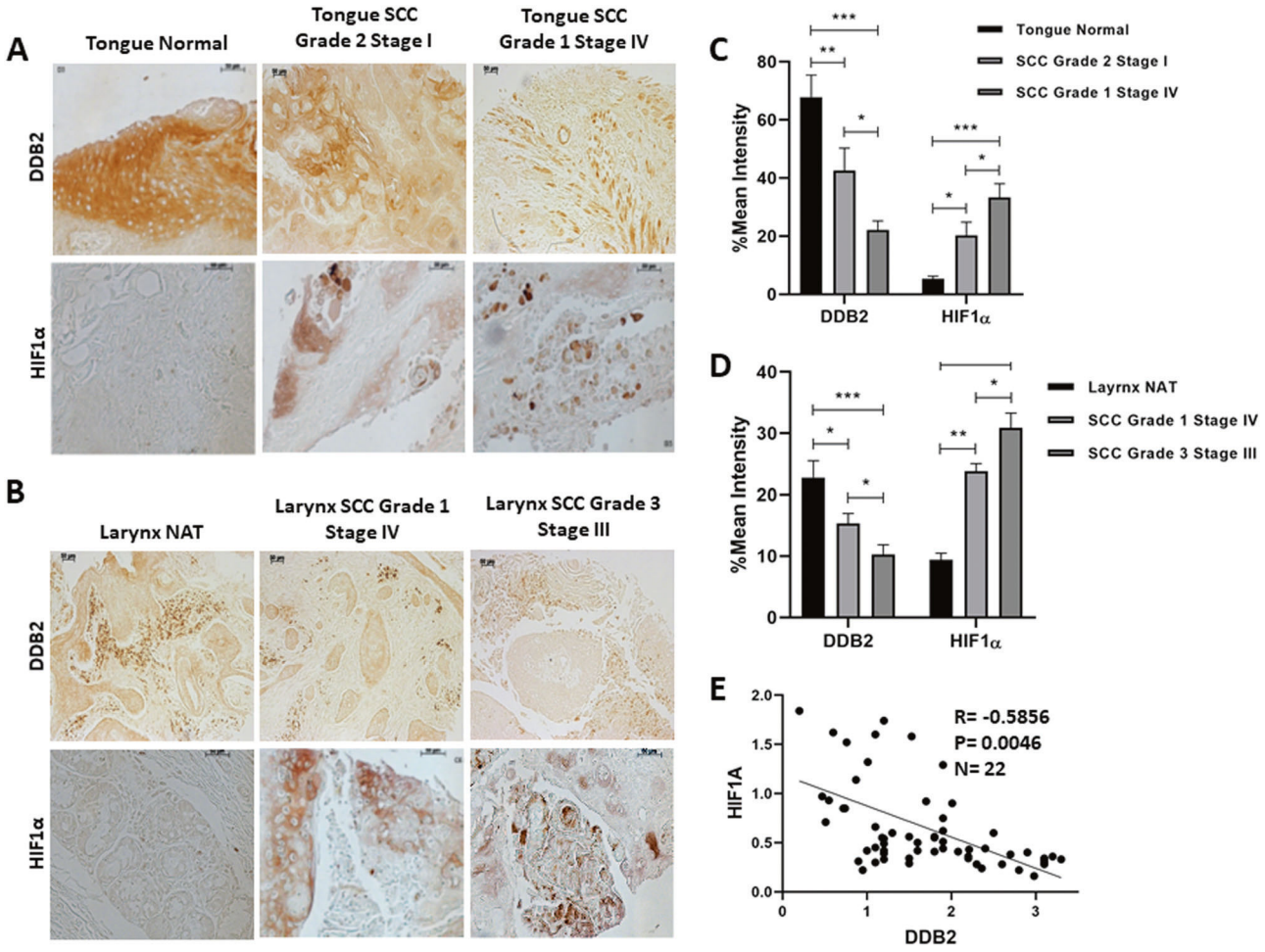

Fig. 6.

Loss of DDB2 and gain of HIF1α expression in HNSCC tumor tissues. Expressions of DDB2 and HIF1α in HNSCCs were analyzed by staining commercially available tumor microarrays with DDB2-Ab and HIF1α-Ab, as described in materials and methods. Representative images of (**a**) normal tongue tissue, tongue SCCs, and (**b**) tumor adjacent normal larynx tissues (NAT) and larynx SCCs are shown. Measurement bar in the images are 50 μm. **c, d** The ImageJ intensity quantification of DDB2 and HIF1α staining. Data are shown as ± SD. One-way ANOVA, **P* < 0.05, ***P* < 0.01. e The Pearson correlation coefficient between DDB2 and HIF1α expression.

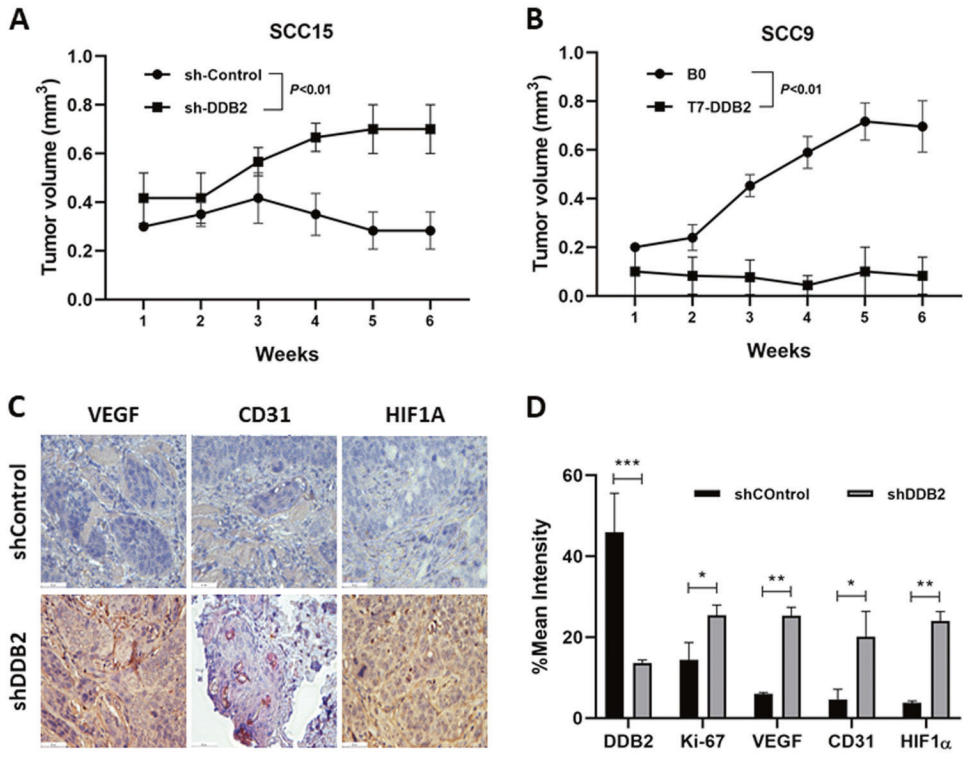

Fig. 7.

DDB2 negatively regulates the tumor progression of HNSCC. A pool of SCC15 cells stably expressing sh-Control or shDDB2 and SCC9 cells stably expressing empty vector (B0), or T7-DDB2 were subcutaneously injected into athymic nude mice and tumor growth were observed for six weeks. **a** The tumor growth curve in mice injected with SCC15:sh-Control and SCC15;shDDB2. **b** Tumor growth curve of mice injected with SCC9:B0 and SCC9:T7-DDB2 expressing cells. Data are shown as ± SD. Students *t* test (Mann–Whitney). **c** Immunohistochemistry was performed on the tumor sections obtained from the xenografts of SCC15:sh-Control and SCC15:shDDB2. Representative tumor sections stained with VEGF-Ab, CD31-Ab, and HIF1α-Ab are shown. Images were captured at ×40 magnification and the measurement bar in the images are 50 μm. **d** The intensity profile of DDB2, CD31, VEGF, Ki67 and HIF1α staining, calculated from at least three images using ImageJ software and the statistical calculation was performed using the Graphpad prism software. Error bars, ± SD. One-way ANOVA, $*P < 0.05$ and $**P < 0.01$. SN (signal to noise) ratio was greater than 3, which generated a power greater than 80% with three mice per sample.